Nano-particle Characteristic Emitted from Gasoline Direct Injection Engine Equipped with Non-Thermal Plasma Device

Pichitpon Neamyou[1,2] , *Kampanart* Theinnoi[1,2,*], *Boonlue* Sawatmongkhon[1,2], and *Sak* Sittichompoo[1,2]

[1] College of Industrial Technology, King Mongkut's University of Technology North Bangkok, 1518 Pracharat 1 Road, Wongsawang, Bangsue, Bangkok 10800, Thailand.
[2] Research Centre for Combustion Technology and Alternative Energy (CTAE), Science and Technology Research Institute, King Mongkut's University of Technology North Bangkok, Bangkok 10800, Thailand.

Abstract. The impact of non-thermal plasma (NTP) on particulate matter (PM) removal, nitrogen oxide (NOx) reduction, and hydrocarbon species in exhaust gases from gasoline direct injection (GDI) engines using gasoline E20 fuel and a mean effective pressure (IMEP) of 6 bar. The experiments were conducted with an exhaust gas flow rate of 20 L/min, applying high voltage in the range of 0 to 10 kV (2 kV per step) at a frequency of 500 Hz. The results show that NTP reduces PM concentrations, particularly in the nucleation mode (10 nm particles). Maximum PM removal of approximately 83% However, with experimental results, compared to 0 kV, the production of particulate matter Aitken mode increased up to 19 times for a voltage increase of 10 kV, and NOx removal has been at a maximum of about 9.5%, with an energy density of 5 J/L at 10 kV. The effects of NTP on hydrocarbon species such as ethylene, propylene, acetylene, 1.3 butadiene, methane, and ethane have been slightly affected by increased high voltages.

Keyword. Exhaust Gas Emissions, GDI Engines, Non-Thermal Plasma, Particulate Matter

1 Introduction

Gasoline Direct Injection (GDI) engines are becoming increasingly popular due to their improved fuel efficiency and performance [1-4]. However, the diffusion combustion in GDI engines leads to emitting high levels of particulate matter (PM) and nitrogen oxides (NO_x), which are harmful pollutants that can have negative impacts on human health and the environment. PM is made up of tiny particles that can penetrate deep into the lungs, causing respiratory problems, and can also contribute to heart disease and other health issues [5-8]. NO_x is a group of gases that can react with other chemicals in the atmosphere to form smog and acid rain, which can harm crops and ecosystems. In addition, GDI engines can also emit other pollutants such as carbon monoxide (CO), volatile organic compounds (VOCs), and sulfur dioxide (SO_2) [9-10]. These pollutants can contribute to air pollution and have negative impacts on air quality and human health. Overall, while GDI engines offer improved fuel efficiency and performance compared to traditional port fuel injection engines, they do emit higher levels of pollutants that can have negative impacts on human health and the environment [11-14]. As such, there is ongoing research and development aimed at reducing the emissions from GDI engines and improving their environmental performance. PM emissions from GDI engines can be a significant concern due to the potential health impacts of these tiny particles.

GDI engines produce PM as a by-product of the combustion process, which can include a range of materials such as carbon, unburned hydrocarbons, and metal compounds. Studies have shown that GDI engines can produce higher levels of PM compared to traditional port fuel injection engines. Fuel is injected directly into the combustion chamber under high pressure, which can cause the fuel to atomize and mix poorly with the air, leading to incomplete combustion and high PM emissions [15-18]. The PM emissions from GDI engines are generally classified into two categories: solid particle emissions and soluble organic fraction (SOF) emissions. Solid particle emissions are composed of tiny particles that can be inhaled deep into the lungs and can cause health problems, such as respiratory issues and heart disease [19-20]. SOF emissions are composed of organic compounds that are soluble in water, which can have negative impacts on water quality and aquatic ecosystems [18].

To control the PM emissions from GDI engines, manufacturers are exploring a range of solutions, such as optimizing fuel injection timing and pressure, using particulate filters, and developing new combustion strategies. In addition, the emission regulators are implementing stricter standards to encourage the development and adoption of cleaner engine technologies [21-23]. Soot is composed of a complex mixture of carbonaceous particles and other materials. The exact composition of soot can vary depending on factors, such as the engine operating conditions, the fuel properties, and

* Corresponding author: kampanart.t@cit.kmutnb.ac.th

the combustion process [24-26]. In general, soot particles from GDI engines can contain a range of materials, including elemental carbon, organic compounds, and trace metals, such as lead, cadmium, and nickel [27-28]. The organic compounds in soot can include polycyclic aromatic hydrocarbons (PAHs), which are known to have negative health impacts, as well as other oxygenated and nitrogen-containing compounds. The formation of soot in GDI engines is influenced by a range of factors, including the fuel-air mixing, the combustion chamber design, and the injection timing and pressure. Soot formation tends to increase at higher engine loads and speeds, and at lean air-to-fuel ratios, where incomplete combustion can occur [29-30]. However, direct injection engines are emitted higher levels of PM emissions compared to conventional port fuel injection engines.

PM emissions from GDI engines can be reduced using after-treatment technologies, such as Diesel particulate filters (DPFs): DPFs can trap and remove PM emissions from the engine exhaust. Selective catalytic reduction (SCR): SCR uses a catalyst to reduce nitrogen oxide (NOx) emissions, which can, in turn, reduce the formation of PM. Exhaust gas recirculation (EGR): EGR reduces the formation of NOx emissions, which can also reduce the formation of PM. Gasoline particulate filters (GPFs): GPFs are like DPFs but are designed specifically for gasoline engines and can trap and remove PM emissions [31-33]. NO_x emissions from GDI engines can also emit NOx because of the high combustion temperatures and pressures. NOx is a term used to describe a group of gases that includes nitrogen oxide (NO) and nitrogen dioxide (NO_2). NO_x emissions can have negative impacts on human health, including respiratory problems, heart disease, and other health issues. Additionally, NOx emissions can contribute to air pollution and have negative impacts on air quality, visibility, and climate change. The formation of NO_x in GDI engines is influenced by factors, such as the fuel-air mixture, combustion chamber design, and engine operating conditions. To reduce NO_x emissions from GDI engines, manufacturers are exploring a range of strategies, such as optimizing fuel injection timing and pressure, using EGR systems, and developing new combustion strategies that promote lower combustion temperatures. Regulations are also being implemented to encourage the development and adoption of cleaner engine technologies that can reduce. the emissions of NOx and other harmful pollutants [34-36].

Nonthermal plasma (NTP) is a technology that uses electrical discharges to produce reactive species, such as ions, radicals, and photons, which can oxidize or reduce pollutants present in exhaust gases. It operates at relatively low temperatures compared to conventional thermal plasma [37-38]. The reactive species produced by NTP can interact with and break down pollutants, including particulate matter (PM), nitrogen oxides (NOx), and volatile organic compounds (VOCs), into smaller and less harmful components. The use of NTP is a promising approach to reduce emissions in different applications, including automotive exhaust after-treatment systems. NTP has been shown to be effective in reducing PM emissions in various types of engines, including GDI engines. In addition to reducing the overall PM mass emissions, NTP has been found to be effective in reducing the number of ultrafine particles (<100 nm) and nanoparticles (<50 nm) emitted from GDI engines. These smaller particles have been shown to have a greater impact on human health than larger PM particles, as they can penetrate deeper into the lungs and even enter the bloodstream. Studies have shown that NTP can reduce PM number emissions from GDI engines by up to 90%. [39]. NTP has also been found to be effective in reducing nitrogen oxide (NOx) emissions from GDI engines. NOx is a major contributor to air pollution and has been linked to a range of health problems. NTP can selectively reduce NOx emissions by converting NOx to nitrogen and oxygen through chemical reactions in the plasma.

The research aimed to investigate the effect of non-thermal plasma technologies on nanoparticle characteristics in exhaust gas emissions from GDI engines fuelled with gasohol E20 fuel. The effect of NTP operating parameters is also investigated in order to improve PM reduction over the different engine operating conditions.

2 Experimental Apparatus

A schematic diagram of the experimental setup is shown in Figure 1. Experiments were conducted on a 1.3 L, four-cylinder, four-stroke, gasoline direct injection engine (Mazda 2, P3-VPS). The engine specifications are detailed in Table 1. The engine operating conditions are engine load was maintained constant at 6 bar indicated mean effective pressure (IMEP), engine speed at 2000 rpm, gasoline E20 fuel in all the experiments. The constant exhaust gas flow rate through the NTP reactor was kept at 20 L/min. the water trap is used to cool exhaust gas to ambient temperature before entering the reactor. In order to prevent blockage and the risk of electrocution, condensate water.

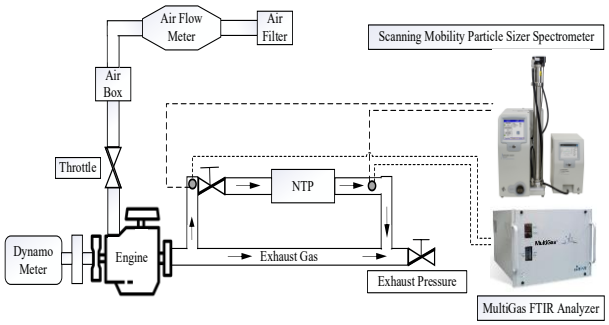

Fig. 1. Schematic diagram of the experimental setup

Table 1. Engine specification of the P3-VPS model.

Engine Parameter	Specifications
No of cylinder	4
Fuel injection	Direct Injection
volume (cm^3)	1298
Bore × Stroke (mm)	82 × 71
Compression ratio	14:1
Maximum power (kW)	62@5400 rpm
Maximum torque (Nm)	112@4000 rpm
Fuel	Gasohol E20

Applying a dielectric barrier discharge (DBD) reactor, plasma was created within the exhaust. DBD is an excellent source of electrons with high energy and density [1]. It consists of an internal and external electrode barrier as shown in Figure 2. Plasma high-voltage amplifier source obtained by Trek 10/10B-HS, Advanced Energy Industries, Inc. Output Voltage: 0 to ±10 kV and Peak AC adjustable from a Digital Oscilloscope DSOX1204G, Keysight Technologies, California, USA. The high-voltage amplifier was used to provide power to the NTP system, while the oscilloscope was utilized to monitor the discharge conditions with applied voltages of 0, 2, 4, 6, 8 and 10 kV at 500 Hz.

In the scanning mobility particle sizer (TSI, SMPS-3082), the size distributions of particles collected before and after the NTP reactor are measured. The particle deposition rate inside the reactor was determined by measuring the PM size distribution at the reactor inlet and reactor exhaust without applying any voltage. The plasma was then introduced into the NTP reactor at the previously described voltage levels. Moreover, the effect of NTP on different nitrogen oxides and hydrocarbon species has been considered. To find out the impact of NTP on NOx concentration, NO, NO2, N2O, and hydrocarbons, which promoted the soot particle, have been measured by the Fourier transform infrared (FTIR) MKS Instruments MultiGas 2030 Gas Analyzers in the reactor with and without High voltage differences.

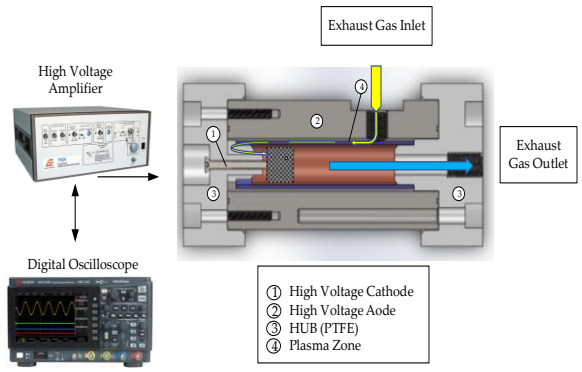

Fig. 2. Schematic diagram of Non-thermal plasma (NTP) system.

3 Results and discussion

3.1 Plasma Discharge power characteristics

The alternating current (AC) voltage generated by increasing the output of the Trek 10/10B-HS transformer (Advanced Energy Industries, Inc.,) at a frequency of 500Hz, was utilized to create a plasma reaction within the DBD reactor by applying it between two electrodes. The transformer converts the input voltage into high voltage in the range from 0 kV to 10 kV (high voltage, ratio 1:1000). A high-voltage and current probe are built into the transformer (Figure 2) with a ratio of 1 V/1000 V for voltage and 1 V/4 mA for electric current and they are inserted into the circuit to minimize load on the oscilloscope. A digital oscilloscope is used to measure, and data log the discharge power in the NTP reactor (Figure 3). The condition example of 6kV for voltage and 30 mA for voltage amperes is shown in Figure 3. The voltage was 0 kV for the first experiment, and it increased up to 10 kV. The power discharge under different voltages is shown in Figure 4. The experiment found that the low discharge power (0.148 joules) at 2 kV. However, when the higher voltage shown the discharge power steeply increases, especially after 10 kV. At this point, plasma can be maintained. This can be confirmed high free radicals' ions and electron impact reactions inside the reactor.

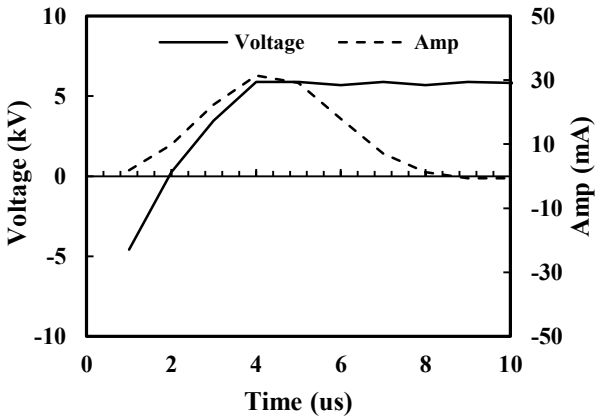

Fig. 3. Voltage and Current signal on oscilloscope

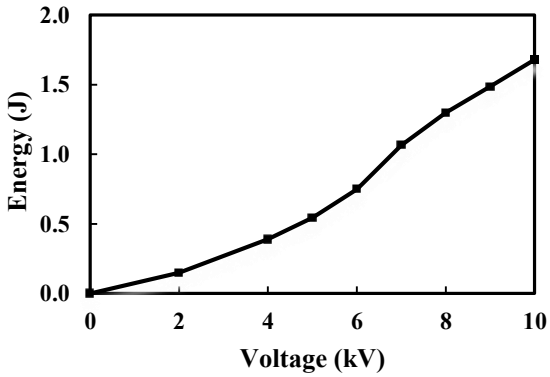

Fig. 4. The effect of voltage on Power discharge for NTP

3.2 Effect of plasma discharge on Particle size distribution

The effect of NTP at different voltage levels is shown in Figure 5. The particle size distribution was measured at the downstream of reactor for all conditions. The result showed that the voltage increases to 2 kV and there is a decline in particle number in nucleation mode (NM) compared to PM numbers from engine out (0 kV). For particles with a diameter range of 10 nm, The NTP reactor exhibited a particle number removal efficiency of 40%. The voltage between 4 kV to 6 kV, the result obtained the particle number removal efficiency of 59% to 65%. After 8 kV, the small particles (<10 nm) have been removed about 80-83% (Figure 6).

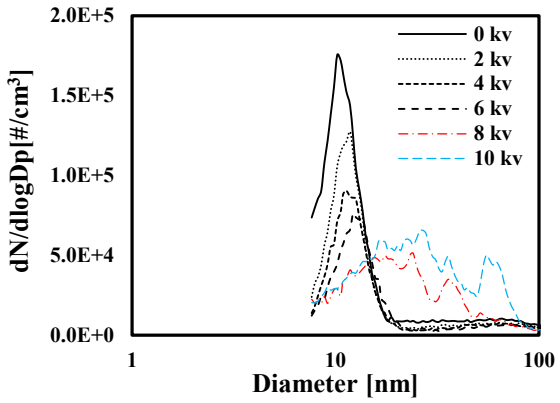

Fig. 5. SMPS particle size distribution at different voltage levels.

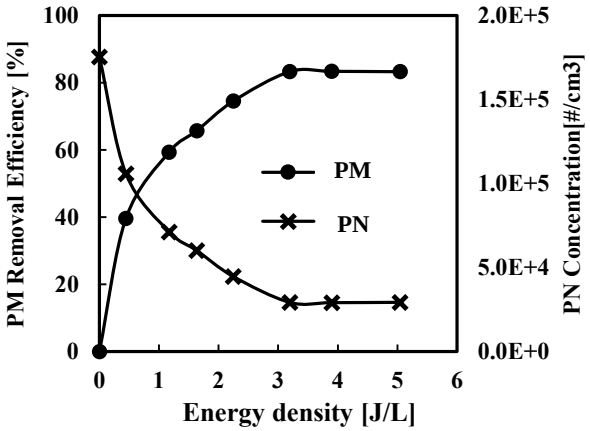

Fig. 6. Effect of energy density on PM removal efficiency and PN concentration.

However, high numbers of particle concentrations in Aitken mode (AKM), particle specific size range of atmospheric aerosol particles with diameters typically ranging from 10 to 100 nanometres, were found at this voltage level. PM size distribution peaks to 6.34 x 10^4 particles, which is 19.5 times greater than the maximum particle number in engine out exhaust gas. In the experiment, it was found that the total PN concentration was in the range of 8 to 10 kV, with a significant increase in nucleation mode and Aitken mode, as shown in Figure 7. In addition, Aitken mode particles are generated through the condensation of SOF that originates from the nucleation mode particles, after the oxidation of their embedded elemental carbons. These particles can also be formed through condensation from the gas phase. The result showed that the main acetylene gas from the NTP reactor had a higher content (Figure 13), when the voltage got to 8 and 10 kV, which was the precursor of soot formation. Subsequently, acetylene gas condenses and combines with small dust particles in the exhaust gases, resulting in the soot formation. The production of acetylene from methane is categorized as a plasma-chemical process, as proposed by Stijn Heijkers and Annemie Bogaerts [46]. In their work, the authors developed a comprehensive chemical kinetics model to investigate the primary conversion mechanisms involved in transforming CH_4 into crucial hydrocarbons, namely C_2H_2, C_2H_4, and C_2H_6, as well as H_2. This analysis encompassed the three prevalent plasma reactors, namely dielectric barrier discharge (DBD), microwave (MW), and gliding arc plasma (GAP) reactors.

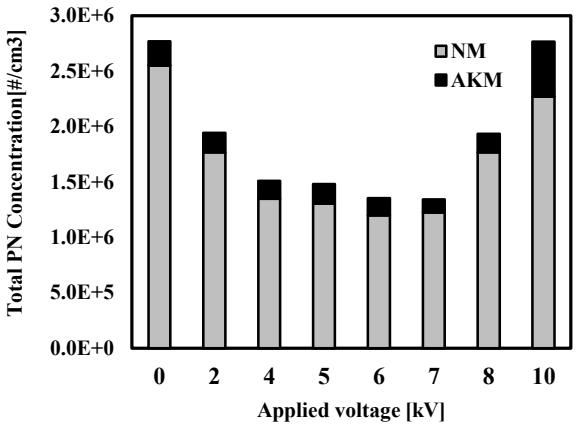

Fig. 7. Comparison of particle distribution of nucleation mode and Aitken mode at different voltage

3.3 Effect of NTP on NOx concentration

The effect of non-thermal plasma on nitrogen oxides has been investigated. The research included adjusting the applied voltages from 2 kV to 10 kV, consistent with previous experimental conditions. The concentrations of NO, NO_2, N_2O, and total NOx ($NO+NO_2$) were considered as shown in Figure 8. The initiation of concentration alteration occurred after applying a voltage of 6 kV. Therefore, plasma beam has low power to handle variations in nitrogen oxide concentrations before this point. The oxidation of NO to NO_2 is explained by the presence of different active oxygen species and ozone. Using a maximum voltage of 10 kV during the experiments resulted in a decrease of approximately 11% in NO concentration and an increase of approximately 48% in NO_2 concentration as shown in Figure 8, similar to previous research that used diesel exhaust gas [44-45].

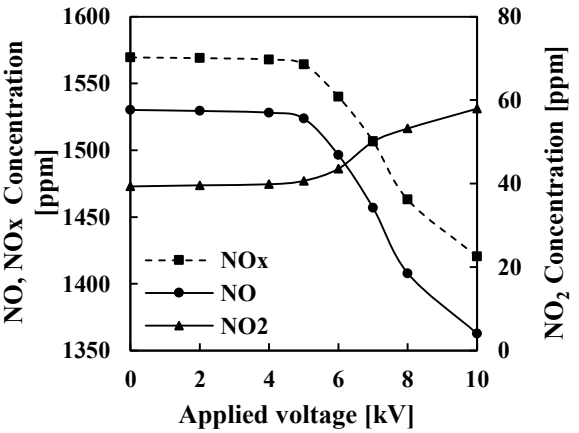

Fig. 8. Effect of non-thermal plasma on nitrogen oxides.

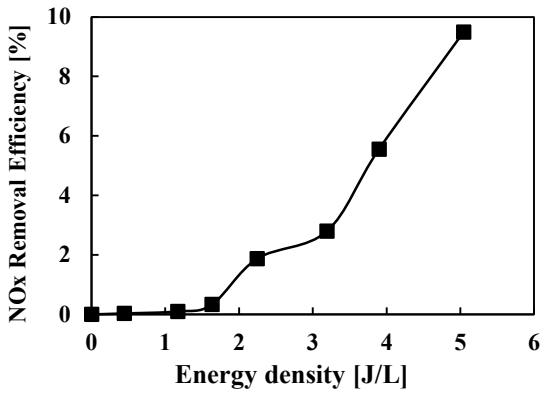

Fig. 9. NO_x removal efficiency at different energy densities.

Figure 9 shows the impact of non-thermal plasma on the NO_x reduction. The maximum value of energy density is constrained by the applied voltage at 10 kV. The discovery has been made that increasing the energy density results in a continuous improvement in the efficiency of NOx removal. In addition, the higher NOx reduction has been observed by increasing the energy density to 5 J/L. For the given configuration, the maximum NOx removal efficiency achieved 9.5% with the energy density was about 5 J/L. The effects of NTP on the different NO_x emissions are shown in Fig 8. The total concentration of NO_x is reduced as the applied voltage is increased. Due to the occurrence of a series of reactions in a plasma state. NO can be removed through equations Eq. (1) and Eq. (2), and it can be oxidized to NO_2 through equations Eq. (3) and Eq. (4), The NO_2 is increased by reaction as shown in equations Eq. (3) and Eq. (4). Moreover, the reduction in NOx concentration can be attributed to the decrease in NO concentration as per equations Eq. (1) and Eq. (2) owing to the significant concentration of NO in the exhaust emission.

$$NO+N \rightarrow N_2+O \quad (1)$$

$$N_2(A)+NO \rightarrow N_2+N+O \quad (2)$$

$$NO+O \rightarrow NO_2 \quad (3)$$

$$NO+O_3 \rightarrow NO_2+O_2 \quad (4)$$

3.4 Effects of NTP on total hydrocarbons (THC) and CO emissions

The NTP effect on total hydrocarbons (THC) concentrations was shown in Figure 10. In this chart, the total concentration of hydrocarbons constantly decreases as the applied voltage increases at 10 kV, and the concentration of THC decreases by around 7%. The reduction of THC can be explained by reaction Eq. (5) to Eq. (8).

$$C_xH_yO_Z + O_2 \rightarrow CO_2 + H_2O \quad (5)$$

$$C_2H_4 + e \rightarrow C_2H_2 + H_2 + e \rightarrow C_2H_2 + 2H + e \quad (6)$$

$$C_2H_4 + O \rightarrow CH_3 + HCO \quad (7)$$

$$C_2H_4 + OH \rightarrow HOCH_2CH_2 \quad (8)$$

The higher voltages cause the concentration of CO to increase as shown in Figure10, but the concentration of CO_2 is not different (Figure11). With respect to the amount of oxygen content in the exhaust, hydrocarbons and soot were converted to CO more than CO_2**.** This is due to the presence of the OH radical in ethanol-blended fuel (E20) as well as the increase in free radicals (OH) resulting from the dissociation of H_2O in Eq. (9). This free radical promotes the conversion of CO through reaction Eq. (10)

$$H_2O + e - \rightarrow OH + H \quad (9)$$

$$CO + OH \rightarrow CO_2 + H \quad (10)$$

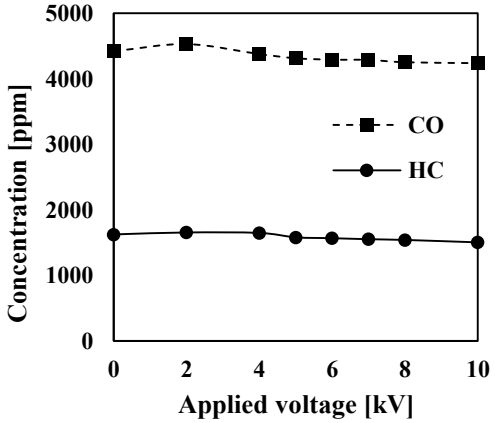

Fig. 10. Effect of NTP on HC and CO Emissions.

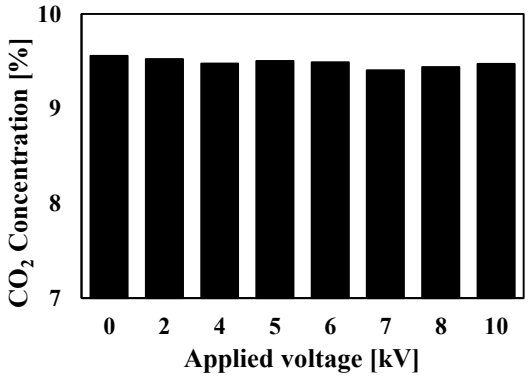

Fig. 11. Effect of NTP on CO_2 Emissions.

3.5 Effects of NTP on hydrocarbon speciation

The hydrocarbon species group can be divided into the following: carbonyl group (formaldehyde and acetaldehyde), unsaturated group (ethylene, propylene, acetylene and 1,3 butadiene), and saturated group (methane and ethane). The effects of NTP on these HCs groups are shown in Figure 12 - 14. In the conditions of a 6-10 kV applied voltage, the carbonyl group exhibits an increase in acetaldehyde (C_2H_4O). The impact of NTP on

formaldehyde (CH_2O) is negligible as shown in Figure 12. This mechanism can be explained as follows: the plasma-generated O, OH, and O_3 species have reactions with hydrocarbons, allowing the formation of alkyl (R), alkoxy (RO), and acyl (RCO) radicals. Then, the alkoxy radicals, such as CH_3O, react with oxygen and produce formaldehyde [40]. When the NTP is applied at 6-10 kV, it appears that ethylene, propylene, and 1,3-butadiene show a trend toward decreasing. The reduction of ethylene (C_2H_4) is caused by the oxygen atoms, which are produced by NTP. The NTP also enhances the decomposition of ethylene to CH_3 through Eq. (11) and then CH_3 can be oxidized to CH_3O_2 through Eq. (12), which helps the reduction of NO via Eq. (13), as shown in Figure 8.

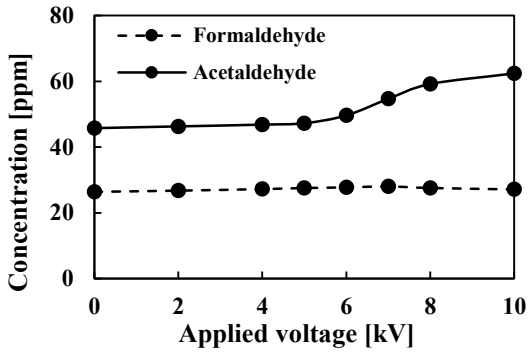

Fig. 12. Effect of NTP on the carbonyl HCs group

However, acetylene exhibits a slight decrease when the NTP voltage is between 0 - 6 kV, followed by an increase when the applied voltage is between 6 - 10 kV, as shown in Figure 13. The increase of acetylene due to the decomposition of ethylene to acetylene (C_2H_2) with NTP by Eq. (14).

$$C_2H_4 + O \rightarrow CH_3 + CHO \quad (11)$$

$$CH_3 + O_2 \rightarrow CH_3O_2 \quad (12)$$

$$CH_3O_2 + NO \rightarrow CH_3O + NO_2 \quad (13)$$

$$C_2H_4 + e \rightarrow C_2H_2 + H_2 + e \quad (14)$$

The effect of NTP saturated HCs group is shown in Figure 14. The NTP has no impact on methane and ethane conversion, because the energy of NTP in the range of 2-10 kV utilized in this study is insufficient to activate transformation of methane and ethane. However, the influence of NTP on the types of hydrocarbons is contingent upon various factors, including the nature of the hydrocarbon, the configuration of the plasma parameters (comprising power, frequency, and gas residence time), and the reactor design. [41-42]. The reactivity of hydrocarbons towards plasma is known to vary depending on their chemical composition, and the reaction could be influenced by a mixture of the different gases in the exhaust gas [43].

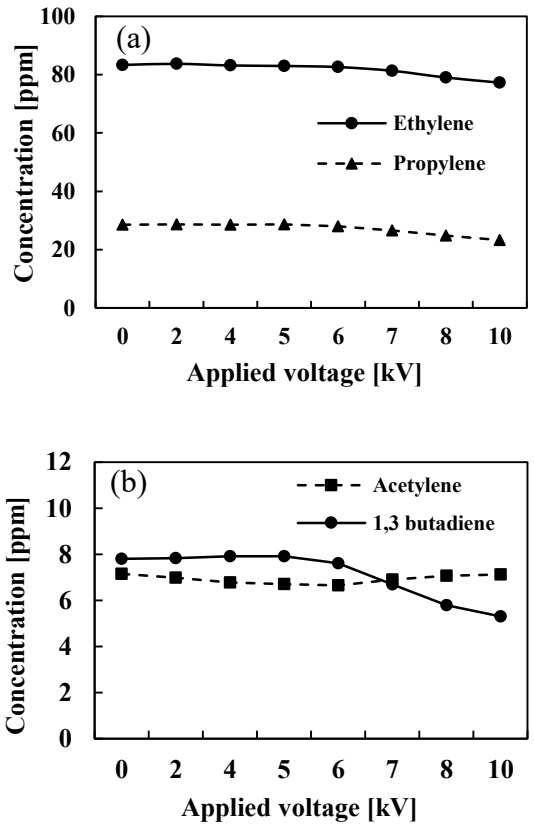

Fig. 13. Effect of NTP on the unsaturated HCs group (a) Ethylene and propylene (b) acetylene and 1,3 butadiene.

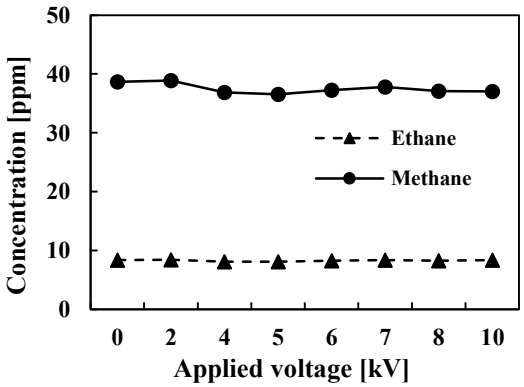

Fig. 14. Effect of NTP on the saturated HCs Group.

4 Conclusion

The effect of non-thermal plasma treatment (NPT) on the distribution of particulate matter (PM) size has been conducted to enhance comprehension of the mechanism of PM removal. NTP can reduce 83% of small particle size (<10 nm), a maximum of 83% with an energy density of 5 J/L. However, the production of particulate matter from 10 nm to 100 nm (Aitken mode) increased up to 19 times for a voltage increase from 10 kV compared with an engine out. Therefore, operating the DBD reactor at 6 kV may be regarded as the ideal operating condition for this design in terms of PM size distribution removal efficiency

and energy consumption in nucleation mode and Aitken mode when considering only the removal of small particulate matter. The effect of non-thermal plasma (NTP) on the size distribution of particulate matter (PM) and nitrogen oxide (NOx) discharge in real exhaust from gasoline direct injection under different voltage conditions. Experimental results show the oxidation of nitrogen monoxide (NO) resulted in the formation of nitrogen dioxide (NO_2). The efficiency of NO_x removal has been shown to be increased with the higher discharge power, reaching a maximum percentage of about 9.5 and the energy density about 5 J/L has been measured. In addition, the different effects of applied voltage on hydrocarbon species, such as ethylene, propylene, acetylene, 1.3 butadiene, methane, and ethane are observed.

Acknowledgements

This research was funded by the National Science, Research and Innovation Fund (NSRF), and King Mongkut's University of Technology, North Bangkok, with Contract no. KMUTNB−FF−66−19.

References

1. A.N. Bukkapatnam, R. Sriramula, Y.J. Kim, Gasoline direct injection engines: Advancements, challenges, and future perspectives, Journal of Energy Resources Technology, **142**,6, (2020): 061201
2. S. Singh, M.R. Golovitchev, A.S.G. Wijewardane, Impact of fuel properties on the spray characteristics and combustion of a gasoline direct injection engine, Energy Conversion and Management, **215** (2020): 112996
3. J. Guo, Y. Hu, Z. Liu, Effect of gasoline direct injection timing on mixture formation, combustion, and emissions in a gasoline direct injection engine, **266** (2020): 117088
4. Y. Zhang, C. Chen, Z. Wang, X. Han, An experimental investigation on the combustion and emission characteristics of a gasoline direct injection engine fueled with hydrogen-enriched gasoline, **246** (2019): 78-86
5. K. Min, M.Y. Kim, D. Kim, S. Kwon, Evaluation of particulate matter emissions from gasoline direct injection vehicles under various driving conditions, Environmental Pollution, **269** (2021): 116180
6. K.H. Kim M.Y. Kim, Emissions characteristics of nanoparticles from gasoline direct injection engines, Science of The Total Environment, **725** (2020): 138293
7. T.D. Durbin, C.R. Bartoli, J.M. Norbeck, Impact of ethanol and aromatic hydrocarbon content on particulate matter emissions from a GDI engine, Energy & Fuels, **33**,3, (2019): 2483-2491
8. F. Yang, C. Xu, Y. Li, H. Xu, L. Li, Influence of gasoline composition and operating parameters on the formation of particulate matter in gasoline direct injection engines, **291** (2021): 120029
9. M. Zheng, G.T. Reader, Nitrogen oxide emissions from gasoline direct injection engines: Mechanisms, control strategies, and future perspectives, Applied Energy, **291** (2021): 116857
10. C.P. Kolodziej, T.D. Durbin, J.M. Norbeck, Impact of fuel composition on the formation and emissions of PM from a gasoline direct injection engine, Environmental Science & Technology, **54**,9 (2020): 5732-5740
11. M. Cheng, L. Hao, L. Li, S. Li, H. Liu, K. Cen, Real-world emissions of non-methane volatile organic compounds from gasoline direct injection vehicles, Science of The Total Environment, **773** (2021): 145565
12. P. Přikryl, M. Vojtíšek-Lom, M. Pohořelý, Particle emissions from internal combustion engines: A review, Atmospheric Environment, **259** (2021): 118482
13. H. Zhang, M. Yao, H. Liu, M. Zheng, Emissions and characteristics of particulate matter from a gasoline direct injection engine at different operating conditions, Journal of Environmental Sciences, **90** (2020): 372-381
14. X. Song, H. Liu, Q. Zhang, Experimental investigation of particulate emissions from a gasoline direct injection engine fueled with gasoline-ethanol blends, **241** (2019): 1056-1062
15. H. Zhang, M. Yao, H. Liu, Investigation of the formation and evolution of particulate matter in a gasoline direct injection engine, **261** (2020): 116433
16. M. Zheng, G.T. Reader, Experimental investigation of particulate emissions from a gasoline direct injection engine during cold-start, **253** (2019): 189-198
17. X. Ma, Y. Xue, H. Zhang, S. Wu, Z. Huang, Effect of injection timing on particulate matter emissions from gasoline direct injection engine under cold-start conditions, **285** (2021): 119023
18. Y. Qiao, J. Cai, J. Lv, B. Liu, Z. Huang, Effect of ethanol blending on the morphology and nanostructure of soot particles emitted from a gasoline direct injection engine, **273** (2020): 117779
19. J. Chen, M. Mousazadeh, A. Sarathy, Characterization of particulate emissions from a gasoline direct injection engine: Influence of operating conditions and fuel components, **261** (2020): 116385
20. G. Zhang, Y. Zhang, Z. Wang, H. Yao, Z. Huang, Effect of engine operating conditions on particulate matter emissions from a gasoline direct injection engine, **260** (2020): 116208
21. A.A. Omidvarborna, A. Ahmed, D.A. Nguyen, G.K. Anderson, In-cylinder particle number evolution in a gasoline direct injection engine, **269** (2020): 117457-117457
22. Y. Qiao, J. Cai, J. Lv, B. Liu, Z. Huang, Effect of ethanol blending on the morphology and

nanostructure of soot particles emitted from a gasoline direct injection engine, **273** (2020): 117779-117779

23. L. Li, C. Huang, Y. Lu, M. Liu, J. Peng, C. Zheng, Effects of fuel injection strategy on soot emissions in a gasoline direct injection engine, Energy Conversion and Management, **242** (2021): 114276
24. S. Zhang, G. Song, X. Huang, Z. Zhang, J. Zhang, Effects of injection strategy on soot emissions from a gasoline direct injection engine during start-up, **233** (2018): 445-454
25. K. Borkar, S.W. King, R.R. Steeper, C.A. Gabrys, Effect of injection timing on soot formation in a gasoline direct-injection engine using in-cylinder imaging, SAE International Journal of Engines, **8**,2 (2015): 1020-1032
26. H. Wu, H. Wang, W. Zhang, Y. Zhang, M. Wei, Effect of injection timing on soot emission and combustion process in a GDI engine, **156** (2015): 97-105
27. J.H. Lee, S. Choi, K. Lee, C.S. Lee, Characterization of particle emissions from a gasoline direct injection engine fueled with ethanol-gasoline blends, IEEE Transactions on Transportation Electrification, **7**,4 (2021): 1516-1523
28. J. Kim, C. Yoo, S. Jeon, H. Bae, Impact of ethanol blend ratio on particulate matter emissions from a gasoline direct injection engine, IEEE Transactions on Transportation Electrification, **6**,3 (2020): 1005-1012
29. S. Shamsudeen, P. Bharath,A. Sivakumar, Influence of fuel-air mixing on soot formation in a gasoline direct injection engine, IEEE Access, **8** (2020): 23756-23764
30. P. Prikhodko, S. Kozlov, D. Kosarev, Effect of injection timing on soot formation in a gasoline direct injection engine, in Proceedings of the 21st International Scientific-Technical Conference on Actual Problems of Electronics Instrument Engineering (APEIE), Novosibirsk, Russia, (2020): 253-258
31. S. Song, S. Gao, W. Yan, J. Zheng, Study on the effect of gasoline particulate filters on particulate matter emissions from gasoline direct injection engines, in Proceedings of the 2021 IEEE Vehicle Power and Propulsion Conference (VPPC), Chengdu, China, (2021): 1-6
32. Y. Lee, S. Kim, S. Han, Investigation of the effect of gasoline direct injection on particulate emissions and after-treatment system performance, in Proceedings of the 2020 IEEE Transportation Electrification Conference and Expo (ITEC), Chicago, IL, USA, (2020): 1-6
33. C. Liu, J. Li, Y. Li, J. Wang, Effect of exhaust gas recirculation on particulate matter emissions from a gasoline direct injection engine, in Proceedings of the 2019 IEEE Vehicle Power and Propulsion Conference (VPPC), Hanoi, Vietnam, (2019): 1-6
34. Y. Liu, Q. Wang, Y. Xu, Z. Li, Experimental investigation on particulate matter reduction by non-thermal plasma in a gasoline direct injection engine, in Proceedings of the 2020 IEEE Transportation Electrification Conference and Expo (ITEC), Novi, MI, USA, (2020): 1-5
35. H. Zhao, S. Yuan, H. Li, Y. Zhang, Experimental study on NOx reduction using non-thermal plasma in a gasoline direct injection engine, in Proceedings of the 2020 IEEE International Conference on Automation, Electronics and Electrical Engineering (AUTEEE), Taiyuan, China, (2020): 1-4
36. W. Zhang, H. Zhao, C. Geng, Experimental investigation on non-thermal plasma assisted NOx reduction in a gasoline direct injection engine, in Proceedings of the 2019 IEEE Transportation Electrification Conference and Expo (ITEC), Novi, MI, USA, (2019): 1-6
37. X. Chen, M. Liu, Y. Zhao, X. Wang, Non-thermal plasma technology for diesel engine exhaust gas treatment: A review, in Proceedings of the 2020 IEEE International Conference on Mechatronics and Automation (ICMA), Xi'an, China, (2020): 1-6
38. S. Park, S. Lee, J. Oh, J. Kim, Evaluation of non-thermal plasma on NOx removal for diesel engine exhaust gas, in Proceedings of the 2020 IEEE International Conference on Plasma Science (ICOPS), Chicago, IL, USA, (2020): 1-4
39. K. Park, J. Kim, J. Lee, Y. Kim, Reduction of ultrafine particles using a non-thermal plasma system for GDI engine exhaust, in Proceedings of the 2020 IEEE International Power Electronics and Application Conference and Exposition (PEAC), Nanjing, China, (2020): 1-5
40. A.D. Srinivasan B.S. Rajanikanth, Pulsed plasma treatment for NOx reduction from filtered/unfiltered stationary diesel engine exhaust, in Proceedings of the 2007b IEEE Industry Applications Conference, New Orleans, LA, (2007): 1893-190
41. E. Delikonstantis, M. Scapinello, G.D. Stefanidis, Low energy cost conversion of methane to ethylene in a hybrid plasma-catalytic reactor system, Fuel Processing Technology, **177** (2018): 26-36
42. T. Nozaki, A. Hattori, K. Okazaki, Partial oxidation of methane using a microscale non-equilibrium plasma reactor, Catalysis Today, **98**,4 (2004): 607-616
43. J. Benedikt, Plasma-chemical reactions: low pressure acetylene plasmas, Journal of Physics D: Applied Physics, **43**,4 (2010): 043001
44. T. Iamcheerangkoon, N. Chollacoop, B. Sawatmongkhon, T. Wongchang, S. Sittichompoo, S. Chuepeng, K. Theinnoi, Promotion of the NO-to-NO2 Conversion of a Biofueled Diesel Engine with Nonthermal Plasma-Assisted Low-Temperature Soot Incineration of a Diesel Particulate Filter, Energies, **15**,24 (2022): 9330
45. K. Yoshida, Diesel NOx aftertreatment by combined process using temperature swing adsorption, nonthermal plasma, and NOx recirculation: NOx removal accelerated by conversion of NO to NO2, Journal of the Taiwan Institute of Chemical Engineers, **44**,6 (2013): 1054-1059

46. S. Heijkers, M. Aghaei, A. Bogaerts, Plasma-Based CH4 Conversion into Higher Hydrocarbons and H2: Modeling to Reveal the Reaction Mechanisms of Different Plasma Sources, The Journal of Physical Chemistry C, **124**,13 (2020): 7016-7030